05

Characteristics of a superconducting single-photon detector shielded by ITO under external electric field conditions

© K.O. Sedykh,[1,2] Y. Suleimen,[3,4] S.S. Svyatodukh,[1,3] S.Yu. Zarutskiy,[4] A.S. Podlesnyy,[4] A.D. Golikov,[2,3] I.N. Florya,[2] V.V. Kovalyuk,[1,2] K.E. Lakhmanskiy,[4] G.N. Goltsman[1,4]

[1]National Research University Higher School of Economics,
109028 Moscow, Russia
[2]National University of Science and Technology MISiS,
119049 Moscow, Russia
[3]Moscow Pedagogical State University,
119991 Moscow, Russia
[4]Russian Quantum Center,
121205 Moscow, Russia
e-mail: ksedykh@hse.ru

Received May 4, 2025
Revised May 4, 2025
Accepted May 4, 2025

In this work, a model of a surface ion trap with radio-frequency (RF) electrodes and a superconducting single-photon detector made of niobium nitride shielded by indium–tin oxide (ITO) at a temperature of 2.2 K was investigated. The amplitude of the radio-frequency signal supplied to the electrodes varied within 0.01−2 V at frequencies of 5−35 MHz. The results of the dependence of the dark count rate and detection efficiency of the single-photon detector on the induced external RF- field with a shielded ITO coating are presented.

Keywords: surface ion trap, superconducting single-photon detector, niobium nitride (NbN), shielding, indium tin oxide (ITO), scalable ion quantum computer.

DOI: 10.61011/TP.2025.09.61926.80-25

Introduction

Currently, various technologies exist for the possible implementation of quantum information processing, based on the manipulation of qubits: superconducting circuits [1], quantum dots [2], color centers in diamonds [3], and others. Among other approaches, one of the most promising is the use of qubits, in which information is encoded in the electronic states of individual ions [4]. The ions are isolated from the external environment and trapped using electromagnetic traps. Planar traps are a promising architecture for building scalable systems due to their compact sizes and integrability with photonic integrated circuits [5].

Initialization and state readout of trapped ions are performed by laser manipulation of the internal states of the ions. Since the excited state of optical qubits is accompanied by fluorescence, then various technologies are used for its detecting: photomultiplier tubes [6], CCD-chambers (CCD — Charge-Coupled Device) [7], etc. Avalanche photodiodes (APDs) [8], which operate at room temperatures and provide the possibility of integration with a surface trap, can also be used to detect the state of the ion qubit. However, despite the individual advantages of each technology, rapid detection of the ion quantum state in a surface trap at room temperature on a chip has not yet been achieved.

Superconducting single-photon detector (SSPD) [9] has already proven itself as a promising candidate for implementing a readout process of the optical qubit excited state [10–12] due to its high detection efficiency over a wide wavelength range and a low dark count rate [13]. Usage of such detectors in an integrated design in surface traps will allow reducing time and increasing ion states readout accuracy compared to other technologies.

Complexity of integrating an on-chip SSPD with surface ion traps is due to the complex electromagnetic and thermal environment created by the trap. The bias current in the detector can be modulated by the external radio frequency (RF) field of the trap, which negatively affects the efficiency of the photon readout process. Besides, in order to achieve the best efficiency SSPD detection efficiency, the superconducting transition temperature of the material must be higher than the surface temperature of the trap (usually about 3−4 K). In [10], the authors demonstrated a surface ion trap for beryllium ions $^9Be^+$ with SSPD made of amorphous Mo0.75Si0.25 with critical temperature of 5.2 K. Ion fluorescence was measured at the wavelength of 313 nm at the temperature of 3.45 K. The potential of the radio frequency field of the trap reached an amplitude of 8.8 V at a frequency of $\sim$ 67 MHz, affecting the SSPD characteristics, while the experimental detection efficiency reached about 48 %.

It is necessary to shield the detector from the influence of the external RF field of the trap to achieve the best

result. Different shielding methods have different effects on the field penetration into the detector, and hence on the detection efficiency. In [11], the authors demonstrated numerical modeling of the RF- field strength of the trap for a niobium-titanium nitride (NbTiN) detector for calcium ions $^{40}Ca^{+}$. The presented modeling considered various shielding methods of the detector from the external RF-field of the trap: deposition of a metal mirror located under the detector; deposition of a metal mesh above the detector; deposition of a shielding coating made of indium tin oxide (ITO). The authors show that the most effective shielding method of the detector is a combination of a metal mirror located under the detector and an ITO shielding coating, which reduce the effect of the RF- field strength of the trap by three orders of magnitude during the modeling. Experimental work has shown that with an applied 54 VRF- field potential at 70 MHz and a temperature of 4–6 K, SSPD detectors can also operate successfully with an efficiency of 40 %–6868 % (at a temperature of 2.5 K).

The present study continues the study [12] and aims to improve the performance of a superconducting single-photon detector made of niobium nitride (NbN) with an ITO shield and a gold (Au) metal mirror for shielding the trap's RF-field. The paper presents the results of dark count rate and detection efficiency measurements for a surface ion trap model.

1. Surface ion trap model with ITO-shielded SSPD

The design of the surface ion trap (SIT) model with radio-frequency electrodes and a superconducting single-photon detector shielded from below by a metal mirror (Au) and a protective ITO coating on top is shown in Figure 1. The superconducting single-photon detector, made of a thin niobium nitride film with a 5–7 nm thickness and a 100 nm width nanowire, has a critical current density of about 5 MA/cm^2. A layer-by-layer topology of the surface trap is shown in Fig. 1, *b*.

Surface ion trap model was fabricated using e-beam and photolithography and plasma-chemical etching. The main steps of the SIT fabrication process included deposition of a superconducting niobium nitride (NbN) film; formation of alignment marks; formation of the SSPD detector active region; formation of gold (with a titanium sublayer) detector contacts; formation of gold (with a titanium sublayer) RF-electrodes; and formation of ITO plugs. More detailed description of the fabrication route for the surface ion trap model with SSPD without ITO deposition can be found in [12].

ITO films were formed by DC magnetron sputtering on the substrate surface. A 100 mm diameter target with an In_2O_3/SnO_2composition in a 90 %/10 % weight ratio was used for the sputtering process. The vacuum chamber was depressurized to the gas residual pressure of below $5 \cdot 10^{-6}$ mbar after loading the samples. The following

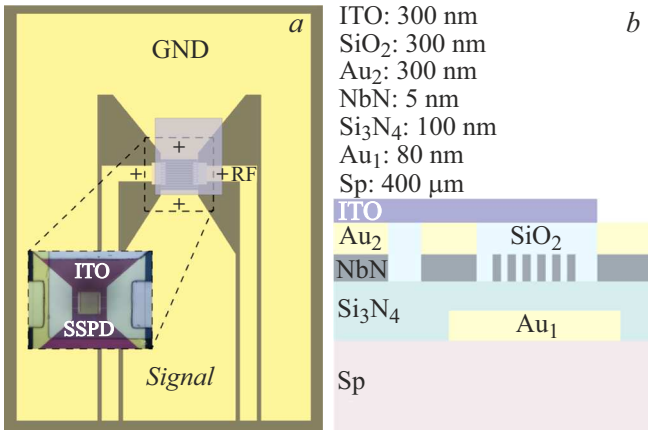

Figure 1. Design of the SIT model with the RF-contacts and SSPD with a microphoto of the detector with 100 nm width nanowire in an optical microscope and a layer-by-layer distribution.

process parameters were selected for sputtering: power supplied to the target — 150 W; the Ar flow — 1 sccm; the chamber pressure during sputtering — $1.5 \cdot 10^{-3}$ mbar. ITO film deposition rate was 25 nm / min with these parameters. The maximum specific power for the ITO target is limited by the heat removal efficiency and should be less than 3.5 W/cm^2 [14]. The thickness of the sputtered films was measured using atomic-force microscopy based on the height difference at the boundary of the ITO structures. The film thickness in experimental samples was defined by a process time based on the measured sputtering rate. Resistance of the ITO sputtered films was studied in a four-probe method.

A metal mirror under the detector is used to shield the detector and reduce the influence of induced RF- currents on its performance. Moreover, the metal shield is an integrated component of a resonator layer designed to increase probability of photon absorption by the superconducting detector. Gold was chosen for this element due to its high reflectivity, while the thickness of the silicon nitride layer corresponds to the wavelength of photons emitted by calcium ions $^{40}Ca^{+}$ [{]15 ensuring high absorption efficiency.

Trapping and cooling of single ions in a surface trap is accomplished using ultraviolet (UV) lasers. The trap's electric field configuration is configured such that the resulting saddle point for ions is located 30–250 μm from the electrode surface. When using free-space optics, UV-radiation effects unavoidably leads to induced charges in the trap's dielectric materials, which complicates the compensation of parasitic electric fields required for ion confinement. It can also cause undesirable heating of the ion due to interaction with the trap's RF-field. To minimize this effect and shield the external RF-field, a visible-transparent ITO layer was used in the experiment; it was grounded during the measurements. However, due to the limitations associated with the conductivity and skin

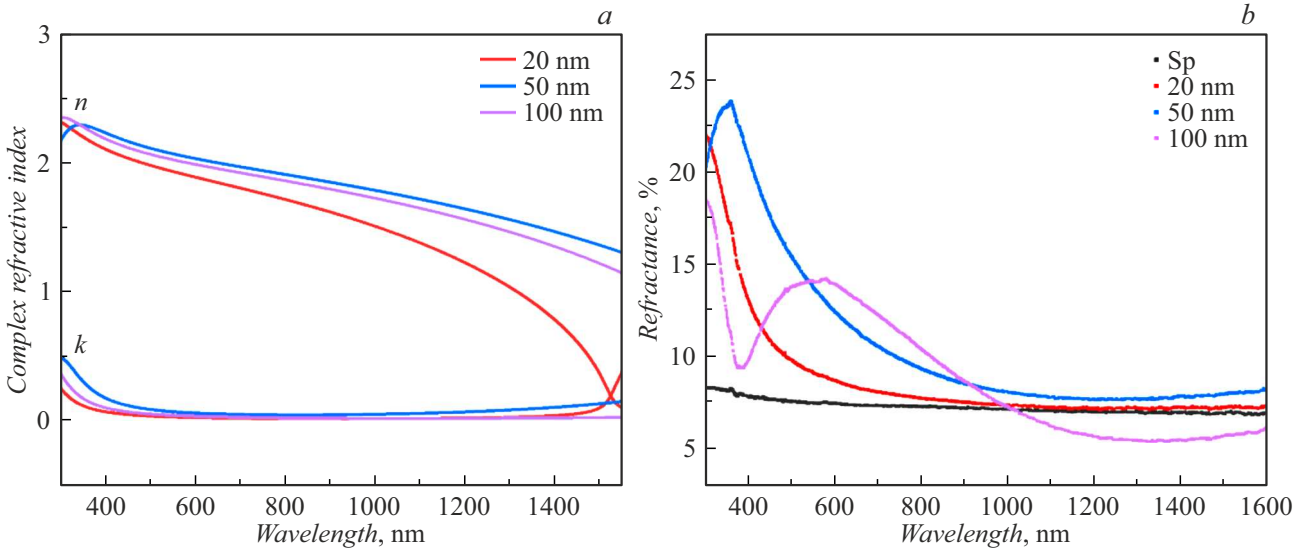

Figure 2. Study of ITO properties: *a* — the dependence of a real (n) and an imaginary (k) parts of complex refractive index of the ITO films on the wavelength for different thickness (20 nm — the red color, 50 nm — the blue color, 100 nm — the violet color); *b* — the dependence of reflectance on the wavelength for the different thicknesses of the ITO films (20 nm — the red color, 50 nm — the blue color, 100 nm — the violet color, Sp — the black color).

effect depth in ITO, future experiments are planned to use a superconducting mesh with a transmittance greater than 90%, which should provide more effective protection against parasitic fields and minimize unwanted heating effects.

ITO layers of different thicknesses (20, 50 and 100 nm) were pre-tested. Fig. 2, *a* shows results of measurements of the dependence of the real (n — the refractive index) and the imaginary (k — the absorption index) part of complex refractive index of the ITO films on the wavelength for the different thicknesses. The measurements were carried out using a Filmetrics setup calibrated using a SiO_2 thin-filmed sample with a known thickness on a silicon substrate In order to increase accuracy of the results, background radiation was subtracted and a pure silicon substrate was as a reference sample as well. The thickness and the refractive index were determined with floating values of n within the wavelength range 200–1600 nm. llumination was provided by deuterium -tungsten and halogen light sources. Fig. 2, *b* shows the dependence of reflectance on the wavelength for the different ITO film thicknesses and sapphire (Sp) as a reference value. Surface resistances of the ITO films on the sapphire substrate were 428, 160 and 82 Ω/□ for the films of the thickness of 20, 50 and 100 nm, respectively. Thicker film was used for further integration with waveguide structures, for local addressing of the ions with the height difference of about 100 nm.

SSPD was mounted on a holder, which was gradually lowered into a cryogenic storage dewar with liquid helium to determine the detector's critical temperature. Resistance-temperature curve was plotted with a characteristic transition of the detector from the normal to the superconducting state as the sample temperature varied. Fabricated detectors had a critical temperature of 7.5 K, which allows measuring the dark count rate as well as SSPD detection efficiency at the temperature of 2.2 K under conditions of the external RF-field.

2. Change in characteristics of the ITO-shielded SSPD under conditions of the external field

The model was studied at the temperature of 2.2 K The main elements of the experimental setup included: a Gifford-McMahon closed-cycle cryostat, a detector bias unit (Scontel), a pulse counter, an external RF-field signal generator, an oscilloscope, and a temperature sensor. The sample installed on a holder plate was placed on a cold cryostat plate and after that the cryostat chamber was depressurized by means of a turbomolecular pump to $\sim 10^{-3}-10^{-5}$ mbar. Then, a cryostat compressor was switched on to cool down the cryostat chamber and the sample to 2.2 K. Bias current in the range from 0 μA to the critical current value ($\sim 15\,\mu$A) was applied to the detector using a bias unit. Detector counts were recorded using the pulse counter (Keysight 53230A) and detector's pulse was simultaneously displayed on the oscilloscope (Tektronix MSO54). External radio frequency field was applied to the corresponding RF- contacts using an arbitrary function generator (Tektronix AFG 31000) with different frequency and amplitude values.

Cryostat's optical input was closed with a special plug to minimize external illumination during dark count rate measurements. The detection efficiency was measured using a supercontinuum laser source (LEUKOS ROCK 400) and a filter (LEUKOS BEBOP), which can be used to control

the wavelength in the range of 450–850 nm and the spectral bandwidth of laser radiation. Cooling of single calcium ions can be achieved using radiation in the visible and infrared ranges, with fluorescence observed at a wavelength of 397 nm. The detection efficiency of the single-photon superconducting detector (SSPD) was measured at a wavelength of 729 nm, corresponding to the qubit transition of calcium ions. With wavelength decreasing, the detection efficiency of the SSPD increases due to a higher photon energy that results in generation of a larger number of the quasi-particles in the superconductor and, therefore, stronger suppression of an order parameter and higher probability of generating a detector response. System efficiency of SSPD is determined by internal efficiency and a photon absorption coefficient. The ultraviolet photons have higher energy compared to the infrared ones, thereby reducing a destruction threshold of Copper pairs and respectively facilitating their detection. Probability of generating a detector response increase, which contributes to an increase in detection efficiency due to the high energy of ultraviolet radiation. Therefore, the obtained detector characteristics at a 729 nm wavelength can be as reference values for assessing the detection efficiency of photons emitted by ions in traps [16].

Optimal trigger level was selected at the beginning of the measurements. It allowed separating a detector's signal from various noises and interference as well as isolating it from the external RF-field of the trap [12]. The selected trigger level (100 mV) was used for the entire series of the measurements. Typically, the RF-signal frequency during operation with specific ions in three-dimensional traps is known and fixed. However, since the research is being conducted in order to integrate the SSPD detector into the surface trap, where ions are located closer to the electrode surface and the fields required for trap operation are lower, it is necessary to find the optimal values for the frequency and amplitude of the external field to match the operation of the trap and detector.

Fig. 3 shows the dependences of dark (open points, a lower part of the graph) and bright (filled points, an upper part of the graph) counts of the SSPD detector with the shielding ITO coating on the bias current. Measurements were carried out in the frequency range of 5–35 MHz (Fig. 3 a–g), including measurements of the characteristics without the induced field of the trap (RF off). The x*x*axis represents the bias current value, the y*y*axis is the number of counts per second. From the obtained results it is clear that the last point of dark counts — the critical current — gradually decreases with external field's amplitude increasing from 14.94 μ A to 14.0μA at a fixed frequency of 5 MHz and from 14.84 μ A to 12.84μA at a fixed frequency of 35 MHz . With increase of the frequency of the external field from 5 to 35 MHz, the value of the critical current decreases from 14.84 to 13.85 μA at the fixed amplitude of 100 mV (Fig. 3, *e*) and from 14.64 to 12.84 μA at the fixed amplitude of 200 mV (Fig. 3, *f*). On the one hand, this phenomenon can be explained the appearance of additional induced RF-currents, which results in increase of probability of the transition of the detector to the normal state. On the other hand, additional charging of the capacitors in the signal pickup circuit occurs, which leads to an increase in the bias current and premature suppression of superconductivity [12].

Analyzing the data presented in Figure 3, it can be noted that the dark count rate does not increase significantly with increasing amplitude of the external RF-field. In comparison with the results presented in [12], where the maximum possible value of the amplitude of the external field of the trap at frequencies reached 800 mV for 5 MHz, in this work it was increased to 2000 mV for 5 MHz. This is a positive result for the integration possibilities of a niobium nitride superconducting single-photon detector to a surface ion trap.

Fig. 4, *a* shows these changes of the critical current in a dependence on the external RF-field. The critical current varies in more than 2 times in the selected range of the fields. The region of the lowest current value can be identified (dark blue region), while in [12] the critical current decreased uniformly with increasing external field values.. The white region in the three-dimensional map shows a not-working region, in which the detector is still in the superconducting state, but the signal readout circuit starts recording the external RF-field. In the study [12], the white region in the three-dimensional map corresponded to a region of the normal state of the detector, in which any measurements are already unavailable.

The detection efficiency of SSPD is defined as a ratio of a number of detected photons per unit time to a number of photons incident on the detector for the same time period. Decreasing in detection efficiency is observed on exposure to external RF-field, therefore, a normalized efficiency is introduced in this work:

$$\eta_N = \frac{N_{field}}{N_{RF_{off}}}, \tag{1}$$

where $N_{RF_{off}}$ and N_{field} is a number of detector's bright counts with RF-field, on and off, respectively, measured at a current value corresponding by 100 dark counts in both cases. To determine the threshold field amplitude (A_{3dB}), at which the detection efficiency decreases twice, the following approximation was used:

$$\eta(A) = \frac{\eta_0}{1 + (A/A_{3dB})^n}, \tag{2}$$

where η_0 is the detection efficiency without a field; A — is the external field amplitude; n — determines curvature of inclination of a power function. The dependence of the normalized detection efficiency on the field amplitude for different frequencies is shown in Figure 4, *b*.

Data characterizing the change in the threshold value of the external field amplitude at a fixed frequency, as well as the curvature of inclination of the function, are presented in Table 1. It is noted that a behavior of the parameters A_{3dB} and n correlates with a change of the detector's critical

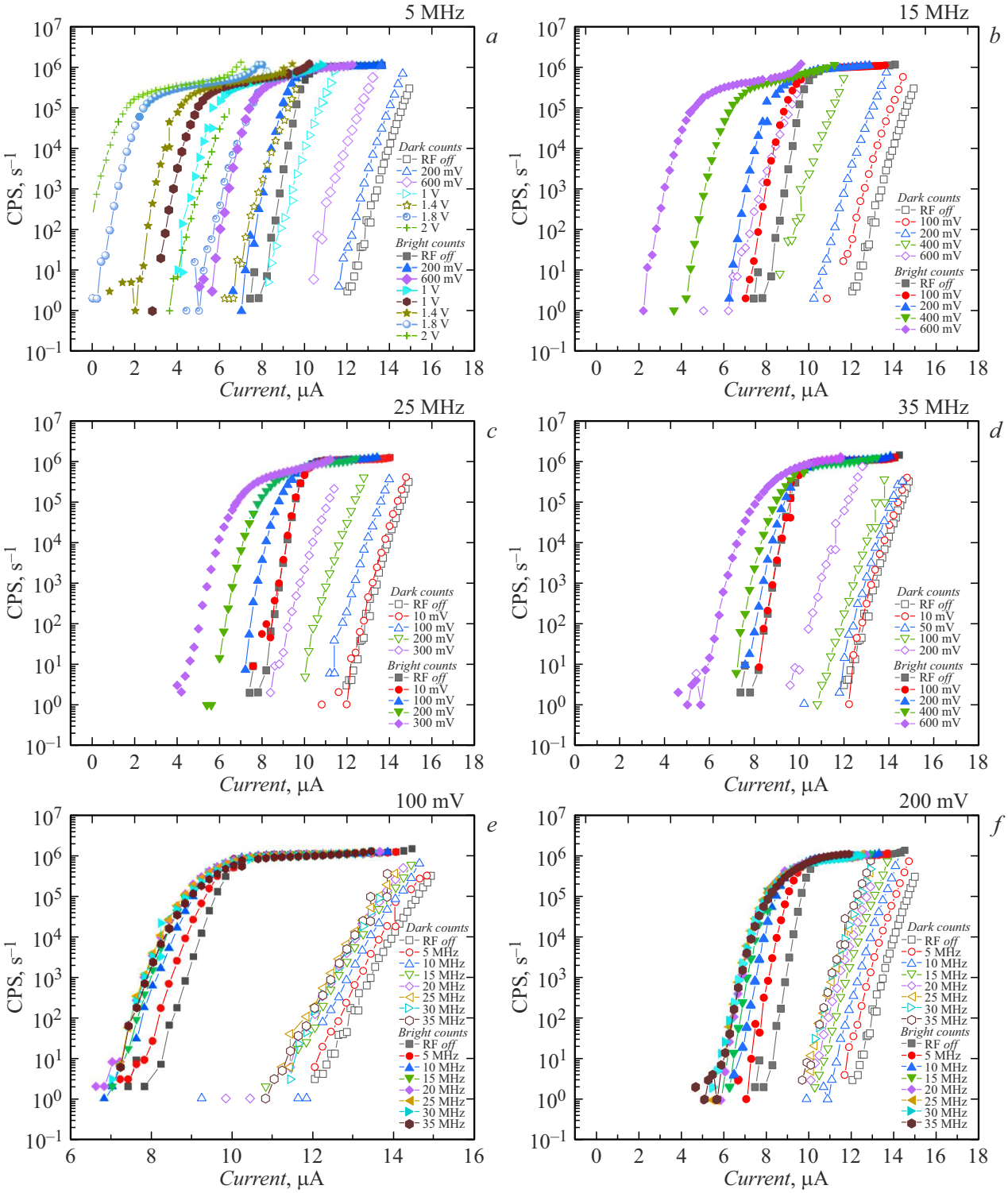

Figure 3. Dependence of the dark (the open markers) and bright (the filled markers) counts of the SSPD detector on the bias current at the different amplitudes and frequencies of the RF-field: *a* — 5, *b* — 15, *c* — 25, *d* — 35 MHz; the dependence for the frequency range 5–35 MHz with the amplitude: *e* — 100, *f* — 200 mV.

current as shown in Fig. 4, *a*. With increasing frequency, the initially high threshold value of the amplitude ($\sim$ 1400 mV at 5 MHz) gradually decreases, reaching a minimum value ($\sim$ 1400 mV at 25 MHz). Further decrease of the threshold amplitude is not recorded due to insufficient data for the frequencies 30 and 35 MHz.

High-speed and high- accuracy single trapped ions quantum state readout is a key challenge in scaling ion trap-based

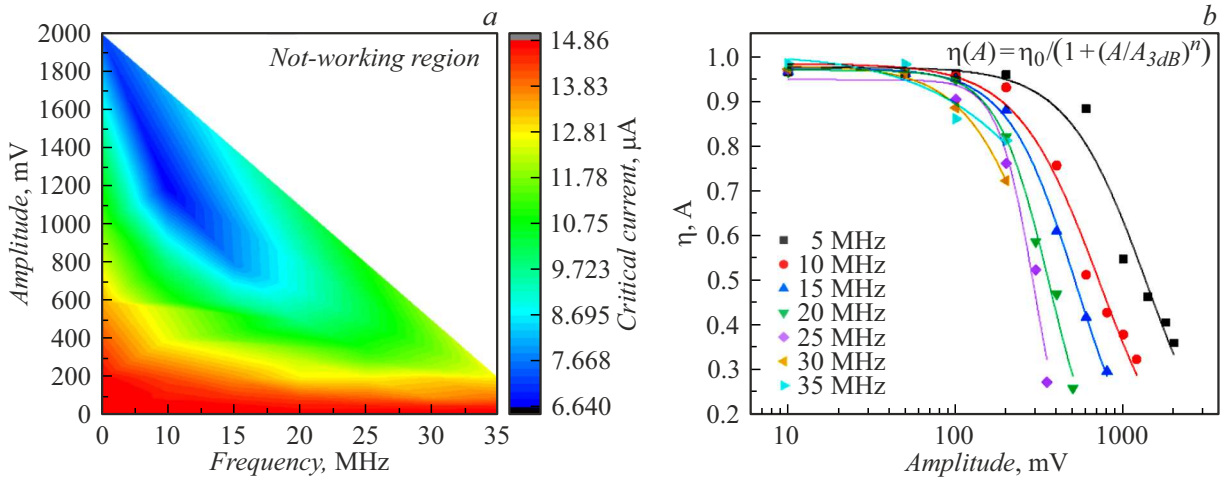

Figure 4. Influence of the external RF-field on the characteristics of the SSPD detector: *a* — the three dimensional map of detector's critical current changes, *b* — detection efficiency.

Values of the external field amplitude parameters at 50% efficiency and the curvature of the inclination of the function depending on the frequency

RF field frequency, MHz	A_{3dB}, mV	n
5	1392.19	1.82
10	726.33	1.75
15	526.38	2.11
20	364.91	2.78
25	296.19	3.97
30	347.58	1.86
35	775.58	1.01

quantum computing architectures. This process is carried out by recording quantum state-dependent fluorescence in the visible range in the visible range with subsequent detection of emitted photons.

Traditional semiconductor photon detectors, including photomultipliers and avalanche photodiodes, provide single-photon sensitivity. However their efficiency is limited ($\sim 30\,\%$) and a high dark count rate ($\sim 6000\,\mathrm{s}^{-1}$) significantly increases the time required to accurately distinguish ion quantum states. Superconducting single-photon detectors (SSPDs), originally developed for the near-infrared range, are being considered as an alternative and can be optimized for detecting ion fluorescence emission. These detectors demonstrate a low dark count rate ($\sim 1\,\mathrm{s}^{-1}$), which is shown in Fig. 3.

When integrating the SSPD directly into the ion trap (with the active area $15 \times 15\,\mu$m), it is necessary to optimize the distance between the ion and the electrodes taking into account thermal effects and a viewing angle that determines efficiency of photon collection. For this purpose, the efficiency of the detector was measured at the different amplitudes and frequencies of the external RF-field Over the distance range of $30-150\,\mu$m, the viewing angle varies within $\sim 0.03\,\%-3\,\%$.

In terms of photon collection efficiency, integration of the detector into a trap structure provides offers no significant advantages over using objectives focusing free-space radiation onto detectors. However, this approach is critical for the scalability of cryogenic surface traps and enables operation of the detector with single-photon sensitivity under cryogenic conditions, significantly reducing readout time compared to alternative methods.

During the readout process, the $^{40}Ca^{+}$ ion emits on average$\sim 2 \cdot 10^7$ photons per second at the $^4S_{1/2} \leftrightarrow {}^4P_{1/2}$. transition. Since the emission of a single ion in the trap is single-photon in nature, the low dead time ($\sim 10\,\mathrm{ns}$) of the SSPD makes it possible to detect successive photons emitted during the readout of the quantum state. This is especially relevant in the context of scalable quantum computations, where an important condition of improving performance is minimization the execution time of a quantum algorithm, including by reducing duration of readout of the quantum state. In ion quantum processors, the readout time is a significant portion of the total quantum cycle compared to the durations of single- and two-qubit operations, as well as the initialization and cooling stages. High single-photon sensitivity, low dead time ($\sim 10\,\mathrm{ns}$) and low SSPD dark count rate allow significantly reducing readout duration. This reduction of the registration time is a key for implementing intermediate measurements within execution of the quantum algorithm, in particular, when implementing quantum correction of error, which requires multiple measurement of the states of auxiliary qubits in real time within a coherency time of the ion qubits ($\sim 1\,\mathrm{h}$ [17]). For a detector with an active area of $25 \times 25\,\mu$m and a system detection efficiency of $\sim 60\,\%$ at a wavelength of 397 nm , with a distance between the ion and the trap electrodes of 30μm , the expected number of detected photons is $\sim 9 \cdot 10^5\,\mathrm{s}^{-1}$. Polarization selectivity of the SSPD

reduces this value to $\sim 4.5 \cdot 10^5\,\mathrm{s}^{-1}$. Due to the single-photon sensitivity of the SSPD and the low dark count rate, the ion quantum state can be read out for the time of less than $10\,\mu$s. Further optimization of the detector which provides the photon detection efficiency above 95% at the ultraviolet wavelength will allow reducing the readout time to $< 1\,\mu$s, which is especially important for the qubit systems.

Conclusion

This paper presents the model implementation of a surface ion trap integrated with a superconducting single-photon detector (SSPD) based on niobium nitride shielded by an indium tin oxide (ITO) coating. The study included the measurements of the dependence of dark count rate on bias current as well as analysis of changes in the critical current and detection efficiency for various external electric field amplitudes in the frequency range of 5–35 MHz at a temperature of 2.2 K.

Sputtering of the shielding ITO coating allowed extending an operating voltage range applied to the surface ion traps electrodes without exit of the detector from the superconducting state up to 2000 mV. Measurement results demonstrate that by increasing the detector bias current and effectively shielding it from RF field effects, the SSPD can be optimized for operation in high PF-field environments.

Further research will be aimed at improving the detector performance by integrating a distributed Bragg reflector optimized for a wavelength of 397 nm, as well as increasing the tolerance to external trap fields by using a superconducting grid with a transmittance of more than 90% and microstrip detectors with a width of $1-10\,\mu$m, the critical currents of which reach $600-700\,\mu$A.

In addition, an alternative method for readout of ion the quantum state using a planar Penning trap is under consideration, in which only static electric and magnetic fields are applied. This approach is expected to significantly reduce the level of induced currents in the detector [18,19].

Funding

The work was supported by the grant FSME-2025-0004 of the Ministry of Science and Higher Education (detectors study) and the federal academic leadership program „Priority 2030“ of the STP „Quantum Internet“ of NUST MISIS (detectors fabrication).

Acknowledgment

The authors would like to tank A. Zaitsev for sputtering the ITO coating.

Conflict of interest

The authors declare that they have no conflict of interest.

References

[1] M. Kjaergaard, M.E. Schwartz, J. Braumüller, Ph. Krantz, J. I.-J. Wang, S. Gustavsson, W.D. Oliver. Annu. Rev. Condens. Matter Phys., **11**, 369 (2020). DOI: 10.1146/annurev-conmatphys-031119-050605

[2] T. Heindel, J.-H. Kim, N. Gregersen, A. Rastelli, S. Reitzenstein. Opt. Photonics, **15** (3), 613 (2023). DOI: 10.1364/AOP.490091

[3] T. Iwai, K. Kawaguchi, T. Miyatake, T. Ishiguro, S. Miyahara, Y. Doi, S. Nur, R. Ishihara, S. Sato. Proceed. IEEE 73rd Electronic Components and Technology Conference (ECTC), 967 (2023). DOI: 10.1109/ECTC51909.2023.00165

[4] J.M. Pino, J.M. Dreiling, C. Figgatt, J.P. Gaebler, S.A. Moses, M.S. Allman, C.H. Baldwin, M. Foss-Feig, D. Hayes, K. Mayer, C. Ryan-Anderson, B. Neyenhuis. Nature, **592**, 209 (2021). DOI: 10.1038/s41586-021-03318-4

[5] C.D. Bruzewicz, J. Chiaverini, R. McConnell, J.M. Sage. Appl. Phys. Rev., **6** (2), 021314 (2019). DOI: 10.1063/1.5088164

[6] A.H. Myerson, D.J. Szwer, S.C. Webster, D.T.C. Allcock, M.J. Curtis, G. Imreh, J.A. Sherman, D.N. Stacey, A.M. Steane, D.M. Lucas. Phys. Rev. Lett., **100**, 200502 (2008). DOI: 10.1103/PhysRevLett.100.200502

[7] R.J. Hendricks, J.L. Sørensen, C. Champenois, M. Knoop, M. Drewsen. Phys. Rev. A, **77**, 02140 (2008). DOI: 10.1103/PhysRevA.77.021401

[8] W.J. Setzer, M. Ivory, O. Slobodyan, J.W. Van Der Wall, L.P. Parazzoli, D. Stick, M. Gehl, M.G. Blain, R.R. Kay, H.J. McGuinness. Appl. Phys. Lett., **119**, 154002 (2021). DOI: 10.1063/5.0055999

[9] G.N. Gol'tsman, O. Okunev, G. Chulkova, A. Lipatov, A. Semenov, K. Smirnov, B. Voronov, A. Dzardanov, C. Williams, R. Sobolewski. Appl. Phys. Lett., **79** (6), 705 (2001). DOI: 10.1063/1.1388868

[10] S.L. Todaro, V.B. Verma, K.C. McCormick, D.T.C. Allcock, R.P. Mirin, D.J. Wineland, S.W. Nam, A.C. Wilson, D. Leibfried, D.H. Slichter. Phys. Rev. Lett., **126** (1), 010501 (2021). DOI: 10.1103/PhysRevLett.126.010501

[11] B. Hampel, D.H. Slichter, D. Leibfried, R.P. Mirin, S.W. Nam, V.B. Verma. Appl. Phys. Lett., **122** (17), 174001 (2023). DOI: 10.1063/5.0145077

[12] K.O. Sedykh, Y. Suleimen, M.I. Svyatodukh, A. Podlesnyy, V.V. Kovalyuk, P.P. An, N.S. Kaurova, I.N. Florya, K.E. Lakhmanskiy, G.N. Goltsman. Tech. Phys., **68** (7), 908 (2023). DOI: 10.61011/TP.2023.07.56637.88-23

[13] K. Smirnov, A. Divochiy, Yu. Vakhtomin, P. Morozov, Ph. Zolotov, A. Antipov, V. Seleznev. Supercond. Sci. Technol., **31**, 035011 (2018). DOI: 10.1088/1361-6668/aaa7aa

[14] Electronic source. Available at: https://www.lesker.com/newweb/deposition_materials/depositionmaterials_sputtertargets_1.cfm?pgid=in3

[15] R. Blatt, H. Häffner, C.F. Roos, C. Becher, F. Schmidt-Kaler. Quantum. Inf. Process., **3**, 61 (2004). DOI: 10.1007/s11128-004-3105-1

[16] Y. Pan, H. Zhou, X. Zhang, H. Yu, L. Zhang, M. Si, H. Li, L. You, Z. Wang. Opt. Express, **30** (22), 40044 (2022). DOI: 10.1364/OE.472378

[17] P. Wang, C.-Y. Luan, M. Qiao, M. Um, J. Zhang, Y. Wang, X. Yuan, M. Gu, J. Zhang, K. Kim. Nat. Commun., **12**, 233 (2021). DOI: 10.1038/s41467-020-20330-w

[18] S. Jain, T. Sägesser, P. Hrmo, C. Torkzaban, M. Stadler, R. Oswald, C. Axline, A. Bautista-Salvador, C. Ospelkaus, D. Kienzler, J. Home. Nature, **627**, 510 (2024). DOI: 10.1038/s41586-024-07111-x
[19] T. Polakovic, W.R. Armstrong, V. Yefremenko, J.E. Pearson, K. Hafidi, G. Karapetrov, Z.-E. Meziani, V. Novosad. Nuclear Instruments and Methods in Physics Research Section A: Accelerators, Spectrometers, Detectors and Associated Equipment, **959**, 163543 (2020). DOI: 10.1016/j.nima.2020.163543

Translated by M.Shevelev